

## Stability Analysis and Performance Evaluation of a Multifunction Converter

Azza E. Lashine<sup>1</sup>, Marwa S. Osheba<sup>1</sup> and Arafa S. Mansour<sup>1,2</sup>

<sup>1</sup>Electrical Engineering Department, Faculty of Engineering, Menoufia University, Egypt

<sup>2</sup>Madina Higher Institute for Engineering and Technology (MHIET), Egypt

(Corresponding author: Marwa.osheba@sh-eng.menofia.edu.eg)

### ABSTRACT

This paper proposes a converter circuit topology that can perform two functions rather than only one function, normally used in the traditional design of Power electronic converters (PEC). Initially the operation of the proposed circuit in boost and inverting modes are outlined. This is followed by the development of a state-space model and extensive frequency-domain and pole-zero stability analyses for the boost mode that give information about the circuit elements requirements and controller design. The proposed converter is simulated using Matlab environment and its performance is evaluated using two control strategies to control the load voltage. The results show the good performance of the converter over a wide range of output voltages and converter capability to reverse the output signal performance and follow the reference values via a logic-based control scheme, which is one of the smart grid application requirements.

**Keywords:** DC-DC converters; modeling; signal analysis; boost converters; average state space modeling .

### 1. Introduction

Power electronic converters (PEC) are gaining more and more interest to process and control the electric energy for user loads. (PEC) mainly deal with the conversion of power from one form to another and the change from one voltage level to multi levels using solid-state switches, such as Power MOSFET, IGBT, ...etc., and relatively lossless components, namely inductors and capacitors [1-3]. Operation of PEC require that the solid-state devices switched on-and-off using many control strategies each of them achieve a specific function. The main function types of Power Electronic (PE) conversion are DC to DC, AC to DC, DC to AC and AC to AC. Each of these functions has its own advantages such as the use of buck-boost converters to step-up or step-down a DC voltage to suit the load requirements, which cannot be achieved using the conventional transformers [4-6].

Traditionally, each of the PEC is designed to achieve only one of the above-mentioned functions. However, the increasing penetration of renewable energy sources and the recent developments in micro-and-smart grids necessitate changing the design philosophy of PEC to perform more than one function rather than one. This is not only for economic reasons but also for operation reliability of the recent developments in micro and smart grids by reducing the number of converters count at lower

cost [12-13]. Multiple DC-DC converters are necessary for not only PV modules to maximize the power generation but also batteries charge. Meanwhile, a bidirectional DC-DC converter that plays a role of charge-discharge regulation for a battery allows flexible power flows in PV systems [7-11]. The work described in the paper is concerned with the stability analysis and performance evaluation of a DC/DC converter

This work described in this paper is a part of a project concerning the development of multi-function power electronic converter (MFC). This paper proposes a converter circuit topology and the control system with the capability of performing two functions as an initial attempt in developing a general purposes MFC. The proposed circuit is analyzed, and the dynamic model is obtained using the state-space approach. The converter stability is extensively analyzed in the frequency and pole-zero domains, and the results are presented. The nature of the converter small signal response and requirements for converter design is demonstrated. A logic-based control system is designed, and the complete system is simulated using the MatLab/SimPower environment. The simulation results are obtained illustrating the response of the positive and negative boost DC/DC converter to pre-specified values. The performance of the converter to changes in load voltage reference is also given.

**2. Circuit Topology of The MFC**

The proposed circuit topology of the MFC is shown in Figure (1). It consists of four power electronic (PE) switches SW1, SW2, SW3 and SW4, an inductor,  $L_e$ , and a capacitor,  $C$ . A logic-based control system is designed and used to enable or disable the PE switches in a way to perform the required functions, according to function setting. For the present two boost functions, the logic-based control system employs four modes of operation; two of them are used to perform positive DC boost while the other two modes of operation enable negative DC boost. The truth table used by the logic-basic controller to operate the converter during the two functions is detailed in Table I. The general dynamic model and the simulation results for the converter operation and performance evaluations are described subsequently.

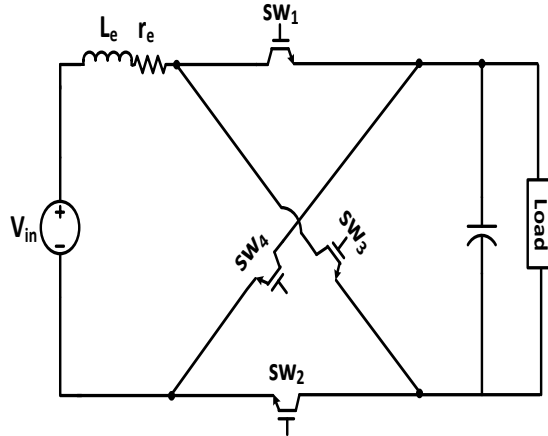


Figure 1- Proposed multifunction circuit topology

Table 1 -The truth table to operate the converter during the two functions

FUNCTION	Operating MODE	SW 1	SW 2	SW 3	SW 4
Positive BOOST	MODE 1	0	1	1	0
	MODE 2	1	1	0	0
Negative BOOST	MODE 1	1	0	0	1
	MODE 2	0	0	1	1

**3. Modelling of DC/DC Converters**

Studying the characteristics of converter under changeable environments such as at starting or when the converter is subjected to sudden changes in loads requires dynamic models of these converters [1]

These models are also important to improve the system transient characteristics via designing the necessary compensator and control systems. In addition, a converter may be used as a voltage regulator or current controller simply by closing a feedback loop between the required output quantity and the duty-ratio of the switching devices. The feedback signal which might be output voltage, output current or input current is compared with a reference for the required control action. The stable operation of the controller relies on the knowledge of the converter's dynamic characteristics and the suitable application of feedback and compensation [1, 14, 15]. This will form difficulty for a switched-mode converter because the converter is highly nonlinear and is controlled by digital type of duty-ratio. This section illustrates a representation of the converter model and shows that the small-signal characteristics of linear systems can be applied successfully to obtain the required dynamic model. The model is obtained and analyzed for the MFC when operating in the DC/DC boost-converting mode.

**3.1 Modeling of the operation Modes**

The operation modes of the multifunction circuit topology, shown in Figure (1), as a Positive Boost (PB) or a Negative Boost (NP) converter are shown graphically in Figure (2). The dynamic equations of the converter can be written for the two operation modes as follows:

**1- Mode 1:**

In this operating mode, the converter circuit during PB and NB functions are Figs. (2a, 2b) where either SW3, SW2 (for PB) or SW1, SW4 (for NB) are closed. The equations that describe the operation during this mode can be obtained as follows:

$$\begin{bmatrix} \frac{di_l}{dt} \\ \frac{di_o}{dt} \\ \frac{dv_c}{dt} \end{bmatrix} = \begin{bmatrix} -\frac{r_e}{L_e} & 0 & 0 \\ 0 & -\frac{R_o}{L_o} & \frac{1}{L_o} \\ 0 & -\frac{1}{c} & 0 \end{bmatrix} \begin{bmatrix} i_l \\ i_o \\ v_c \end{bmatrix} + \begin{bmatrix} \frac{1}{L_e} \\ 0 \\ 0 \end{bmatrix} [V_{in}] \quad (1)$$



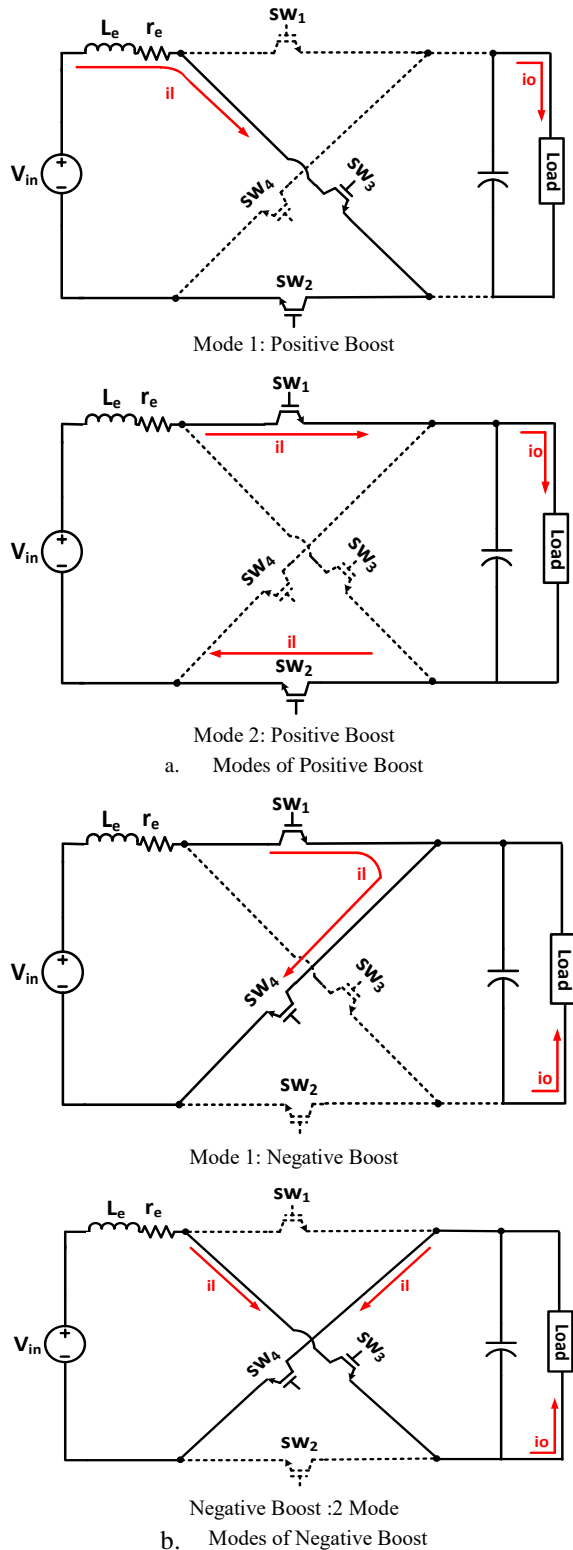


Figure 2- Operation Modes for the DC Boost Function where  $r_e$  and  $L_e$  are the inductor resistance and inductance;  $L_o$  and  $R_o$  are the load resistance and reactance;  $C$  is the converter capacitance.

**2- Mode 2:**

In this operating mode, the converter circuit during PB and NB functions are Figs. (2a, 2b) where either SW1, SW2 (for PB) or SW3, SW4 (for NB) are closed. The equations that describe the operation during this mode can be obtained as follows:

$$\begin{bmatrix} \frac{di_l}{dt} \\ \frac{di_o}{dt} \\ \frac{dv_c}{dt} \end{bmatrix} = \begin{bmatrix} -\frac{r_e}{L_e} & 0 & -\frac{1}{L_e} \\ 0 & -\frac{R_o}{L_o} & \frac{1}{L_o} \\ \frac{1}{C} & -\frac{1}{C} & 0 \end{bmatrix} \begin{bmatrix} i_l \\ i_o \\ v_c \end{bmatrix} + \begin{bmatrix} 1 \\ 0 \\ 0 \end{bmatrix} [V_{in}] \quad (2)$$

**3.2 State-Space Average Representation**

Generally, the time-invariant state-space representation of the continuous conducting modes (CCM) of the converter, Eqs. 1 and 2, can be expressed in the following general form of state-space model:

$$\dot{X} = A \cdot X + B \cdot U \quad (3)$$

When the switching device is turned ON, it conducts for a ratio  $D$  of the duty cycle and consequently the ON mode of operation, Eqn. 1, can be rewritten as:

$$\dot{X} = A_{on} \cdot X + B_{on} \cdot U \quad (4)$$

Similarly, when the switching IGBT is turned OFF, the diode conducts for a ratio of  $(1-D)$  of duty cycle. The state space representation of this period, Eqn. 2, can be rewritten as:

$$\dot{X} = A_{off} \cdot X + B_{off} \cdot U \quad (5)$$

Since the ON-and OFF periods of the converter are represented by the  $D$  and  $(1-D)$  duration periods over the whole duty cycle, Equations 4 and 5 can be averaged by these periods as follows [1]:

$$\begin{aligned} \dot{X} &= [D \cdot A_{on} \\ &+ (1 - D)A_{off}] \cdot X \\ &+ [D \cdot B_{on} + (1 - D) \cdot B_{off}] \cdot U \end{aligned} \quad (6)$$

Equation 6 represent the average nonlinear values of the state variable,  $V_c$  and  $I_l$ , considering all nonlinearities of the converter. However, except for starting the converter operation, variations in duty ratio to match any fluctuations in the controlled output is minimum and represent small deviations in the conduction period. This represent the starting point to apply the small perturbation theory on the overall non-linear state space model, Eqn. 6, about a quasi-operating point, leading to the linear time

invariant state space model that represent the converter dynamical response when subjected to a small changes in the conduction period. Now, consider there is a small signal variation,  $d$ , occurs at the initial duty ratio,  $D_o$ , that will cause a small variation  $x$  of the initial state variables  $X_o$ . This can be written in the form:

$$D = D_o + d \quad (7)$$

$$X = X_o + x \quad (8)$$

Perturbing Eqn. 6 about a quasi-operating point and substitute from Eqs. 7 and 8 yields the following small signal time-invariant state-space model that represent the dynamic characteristics of the converter when subjected to a small deviation  $n$  in the duty ratio:

$$\dot{x} = A . X + F . d \quad (9)$$

where:

$$A = D . A_{on} + (1 - D) . A_{off}$$

and

$$F = [A_{on} - A_{off}] . [B_{on} - B_{off}] . U$$

Using the Matlab symbolic Algorithm, the transfer function with respect to the individual variable can be obtained as

$$\frac{x}{d} = [SI - A]^{-1} . F \quad (10)$$

$$\frac{x}{d} = \frac{\begin{bmatrix} i_l \\ i_o \\ v_c \end{bmatrix}}{d} = \frac{adj[SI - A] . F}{\det[SI - A]} \quad (11)$$

Using the MatLab symbolic Functions reduction, the TF of the converter is obtained as follows:

$$\frac{v_c}{d} = G_o \frac{A_1 S^2 - A_2 S + A_3}{B_1 S^3 + B_2 S^2 + B_3 S + B_4} \quad (12)$$

where:  $G_o$  = Boost converter steady state gain

$$= \frac{V_{in}}{(1-D)}$$

$$A_1 = \frac{-L_e L_o}{(1-D)R_o}$$

$$A_2 = -(1-D) L_o + \frac{r_e L_o}{(1-D)R_o} + \frac{L_e}{(1-D)}$$

$$A_3 = (1-D)R_o - \frac{r_e}{(1-D)}$$

$$B_1 = L_e L_o C$$

$$B_2 = C(L_e R_o + L_o r_e)$$

$$B_3 = r_e R_o C + L_e + L_o(1-D)^2$$

$$B_4 = r_e + R_o(1-D)^2$$

## 4. Converter Characteristics and Stability Analysis

### 4.1 Converter Properties

The frequency response of the converter is obtained in terms of Bode Plot fusing the dynamic model as shown in Figure (3). The result shows almost constant gain at low frequencies before the resonance frequency followed by  $-40$  dB/decade at high frequencies. This indicate poor transient characteristics and requires careful attention in the controller or compensator design [16]. This result illustrates positive phase shift in the phase frequency. This is due to the presence of a Zero in Right-Hand Side (RHS) of the S-plane of the system characteristic equation. Therefore, the results illustrate that the converter transfer function (TF) is called a non-minimum phase system [16]. This term comes from the phase-shift characteristics of such a system when subjected to sinusoidal inputs. This result indicates that the small signal analysis of the converter obeys the following properties of the non-minimum phase systems:

- Non-minimum-phase systems are slow in responding because of their faulty behavior at the start of a response. In most practical control systems, excessive phase lag should be carefully avoided via the introduction of an inner loop to cancel the RHS zero.
- Away from systems that has no RHS zero, non-minimum-phase system will have negative phase and gain margins, which indicate that the correct interpretation of stability margins requires careful study. Therefore, the Root locus of the system is obtained, and the pole-zero diagram is shown in Figure 4b. It illustrates that the converter has two poles at the Left-Hand Side (LHS) of the S-plane and one zero in the RHS. Also, the result illustrate limited range of stability and careful attention should be given to the controller design. The result also shows that increasing the controller gain makes the locus moves from the pole in the LHS to the zero in the RHS while the other pole moves to infinity in the RHS.

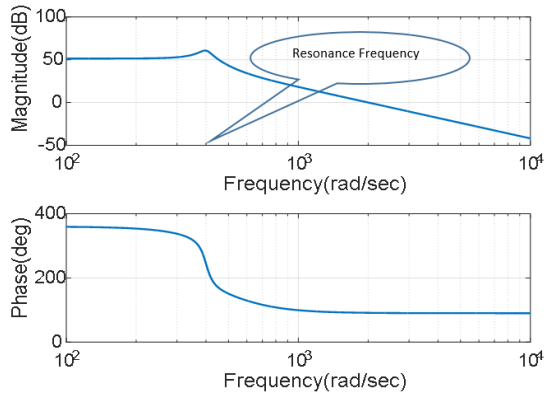
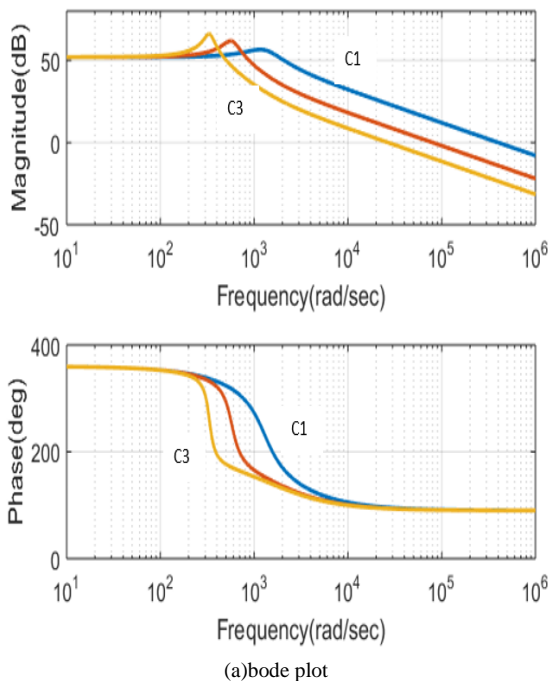


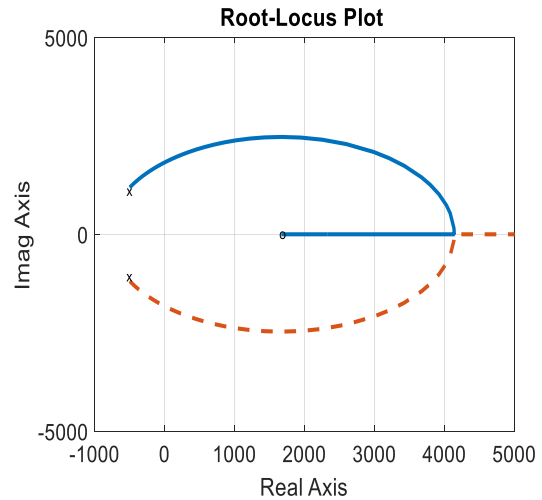
Figure 3- Converter of Bode Plot Diagram

4.2 Effects of varying the converter parameters

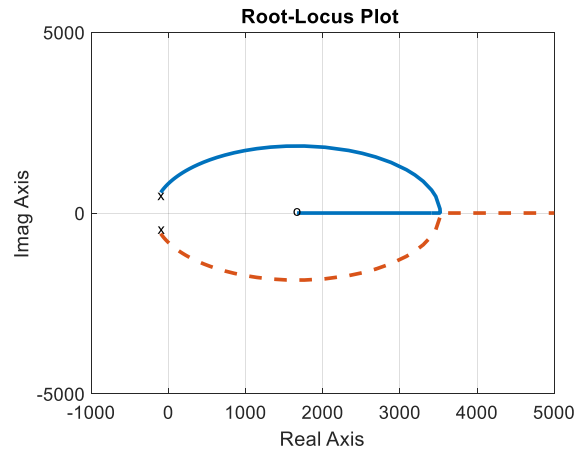
The effects of the varying the converter capacitor on the converter stability at a constant value of the inductor value in terms of frequency response and pole-zero diagrams are shown in Figure (4). The results clearly illustrate that increasing the converter capacitance reduces the stability margin and increases the operating range at high frequencies. Little effects have been observed on converter-damped frequency.



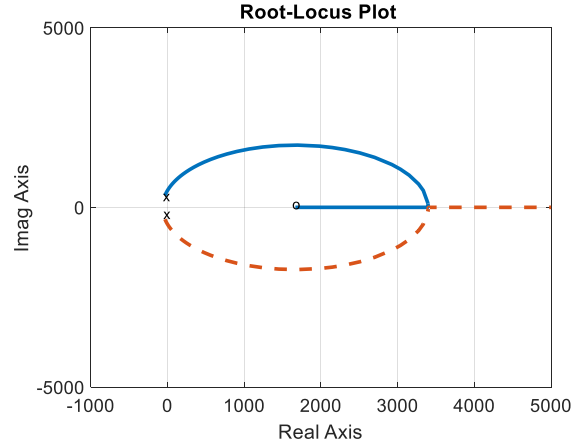
(a) bode plot



$C_1 = 10 \mu F$



$C_2 = 50 \mu F$



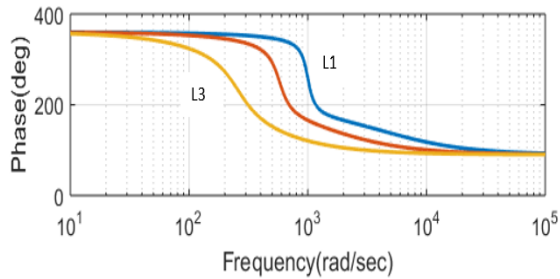
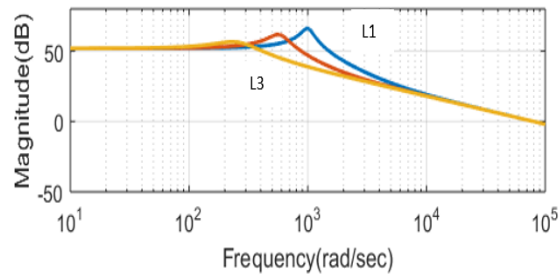
$C_3 = 150 \mu F$

(b) Root Locus

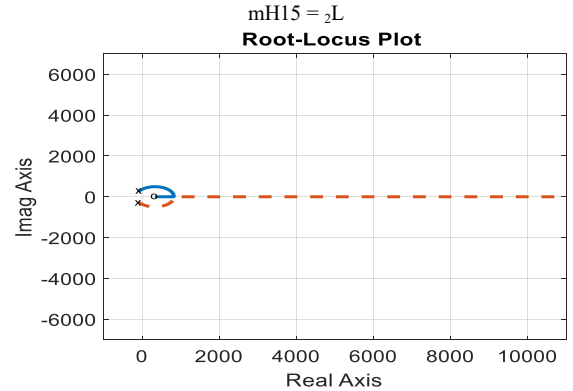
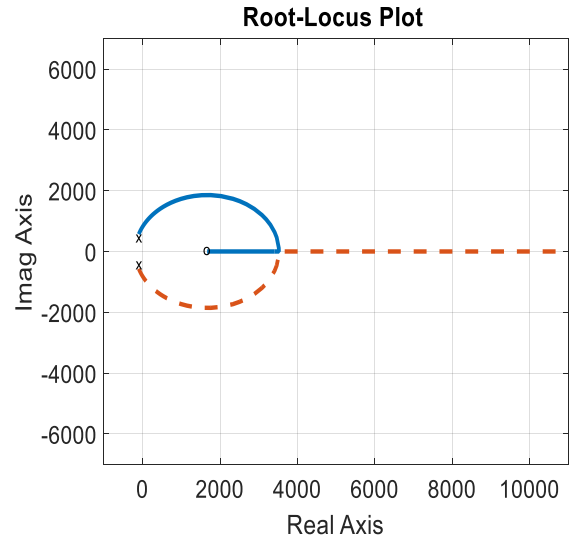
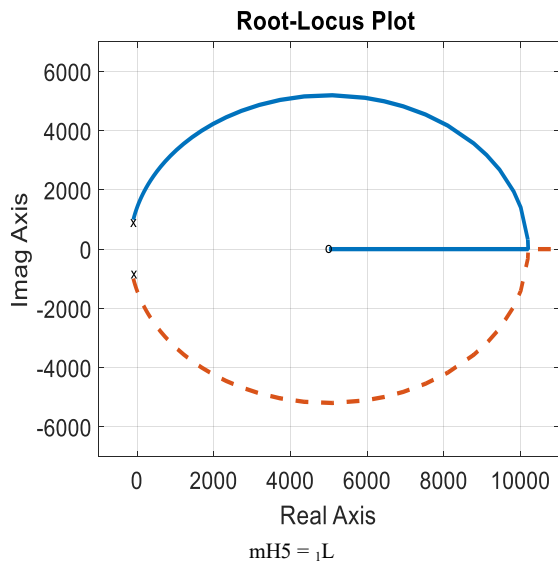
Figure 4- Effects of varying converter capacitance

Moreover, the effects of varying the converter inductance on the converter stability at a constant value of the converter capacitance in terms of frequency response and pole-zero diagrams are

shown in Figure (5). The results clearly illustrate no significant effects of the inductance on converter stability with minor increase of the operating range at higher frequencies. However, a significant effect on the damped frequency is observed with the increase of the converter inductance.



(a) Plot-Bode



(b) Root Locus

Figure 5- Effects of varying converter inductance

### 5. Simulation Results and Performance Evaluation

A detailed simulation is built using the MatLab/SimPower environments and the converter performance is obtained under various conditions to evaluate the DC/DC boosting function in producing a fully controlled output voltage. A signal is feedback from the output voltage and compared with the reference value and the error signal is then compared with a generated sawtooth signal and the resulting signal is fed to the control system as shown in Figure (6). The operation of the MFC in all claimed functions obey the sequence given in the truth table given in Table I, where the MFC power circuit is that shown in Figure 1. The PI controller is designed using Niclus-Zeglar method to determine the initial gain values as described in [16]. The gains are then fine-tuned using trials and errors due to the high non-linearity of the converter and sampled data action. The performance is obtained and demonstrated in the following cases:

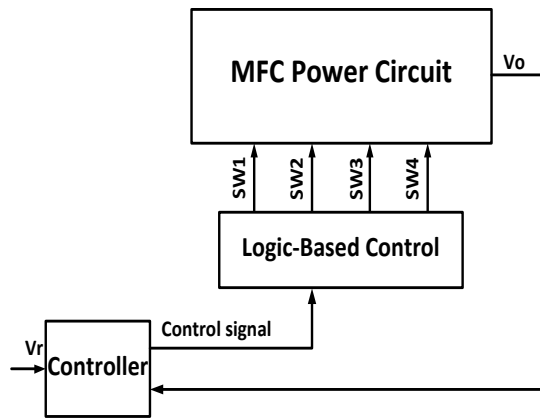
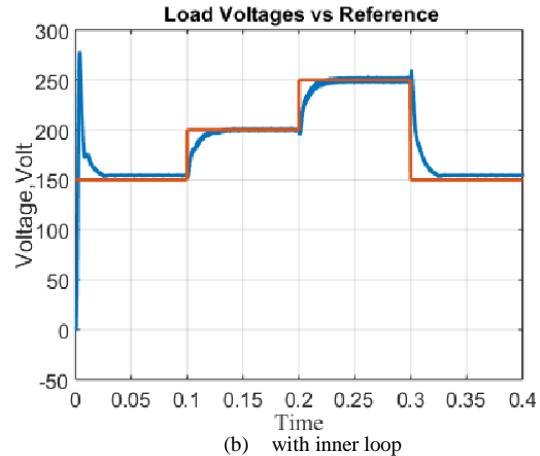


Figure 6- Converter operation using direct voltage control

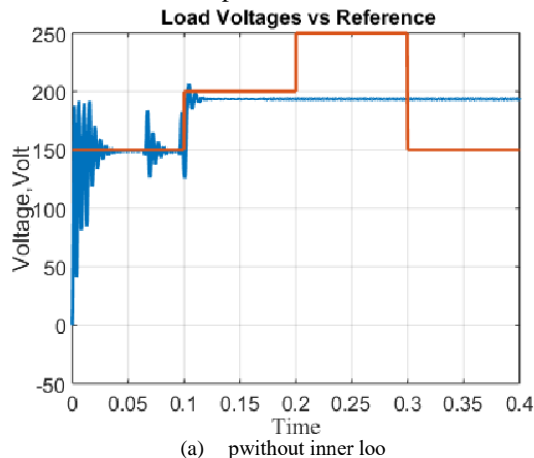


(b) with inner loop  
Figure 7-Response to successive changes in voltage reference

5.1 A- Converter Performance using a PWM-based control structure

1) Response to changes in voltage reference

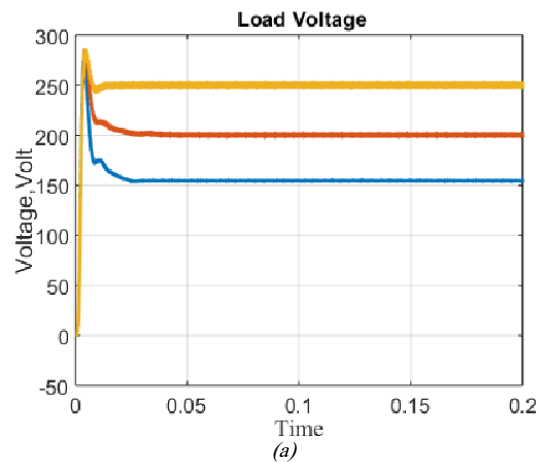
Figure 7a shows the response of the converter at starting and then successive changes in the voltage reference. The results illustrate unsatisfactory performance not only at starting but it also when the converter is subjected to changes in the reference voltage. This could be explained with the aid of the dynamic analysis that indicated that the nature is a non-minimum phase system where a large phase angle exists between the input and output. In addition, the linear analysis indicated the limited range of stability region, which makes the system more sensitive to changes in the system. One of the suggestions to solve this problem is establish an inner loop that eliminates the zero in the TF and lead to more stable and less parameter sensitivity of the system. Therefore, an inner loop is established via a current signal from the inductor current, the test is repeated, and the result is shown in Figure7b that illustrate significant improvements when the system involves an inner loop.



(a) without inner loop

1- Performance of Positive and Negative boost, PWM plus with an inner loop

Figures (8) and (9) show the converter starting performance during positive and negative boost function. The converter reference is set 150 %, 200 % or 250 % of the supply voltage and the converter response to these values and their references are shown in Figures. (8),(9). These results illustrate successful operation of the converter in producing precise control of the output voltage using the PWM and an inner loop from the inductor current.



(a)

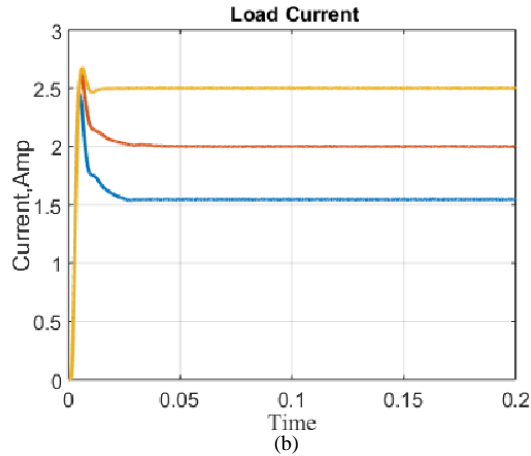


Figure 8-Starting response to 150 %, 200 % and 250 % of supply voltage (Positive Boost ): (a) Load voltage, and (b) Load current

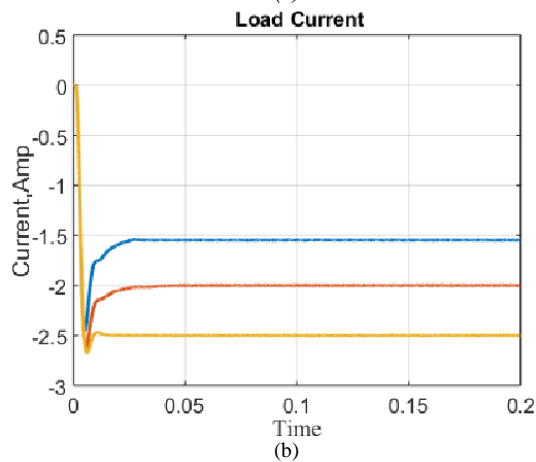
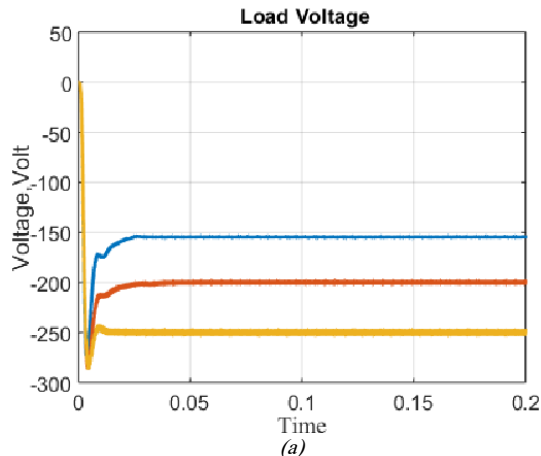


Figure 9-Starting response to -150%, -200% and -250% of supply voltage ( Negative Boost ): (a) Load voltage, and (b) Load current

### 5.2 Converter Performance using a Hysteresis control

The performance of the converter using Hysteresis control is shown in Figures. (10-13). These results

also illustrate the output is well controlled and the logic-based controller is able to operate the converter successfully during positive and negative functions. Also, the results illustrate the ability of the converter to produce precisely the required outputs

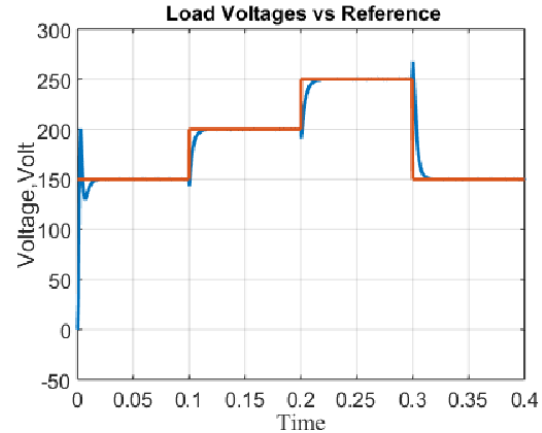


Figure 10-Response to successive changes in voltage reference with inner loop

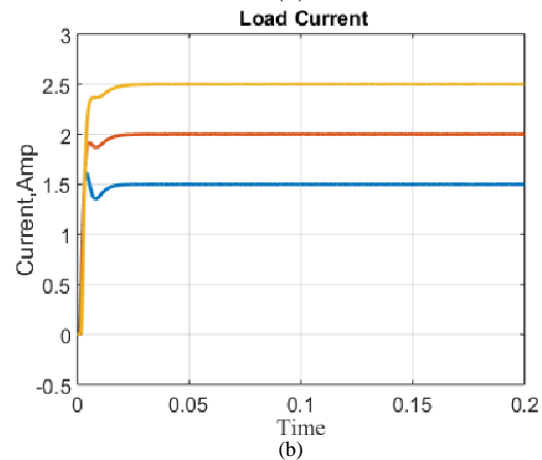
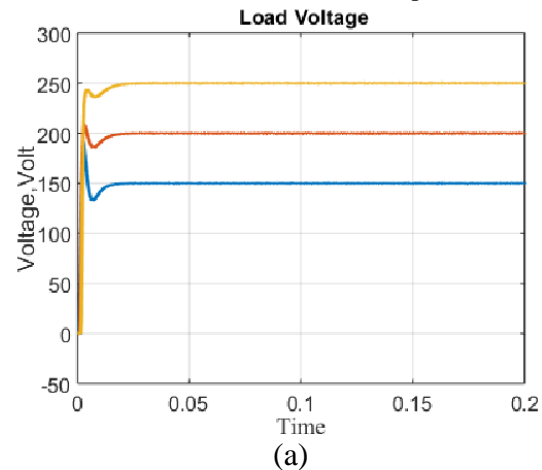


Figure 11-Starting response to 150 %, 200 % and 250 % of supply voltage (Positive Boost): (a) Load voltage, and (b) Load current

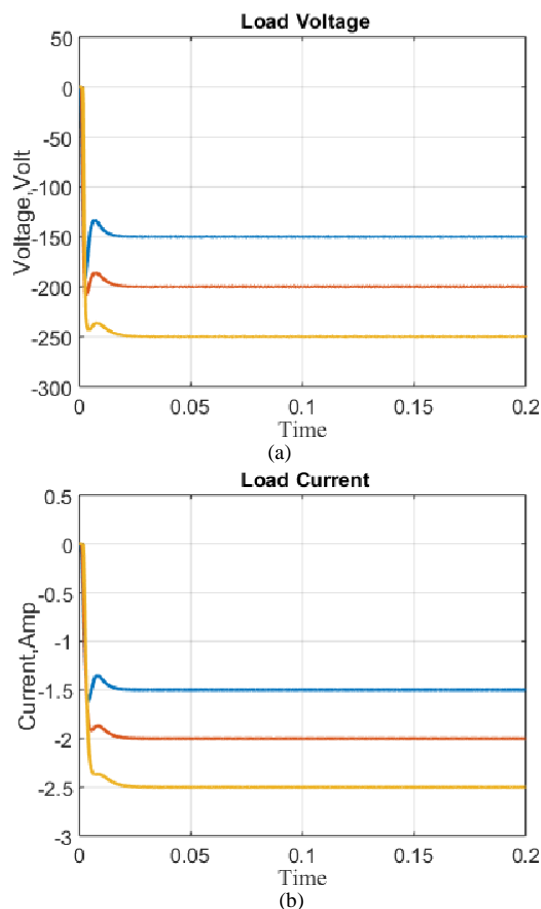


Figure 12- Starting response to 150 %, 200 % and 250 % of supply voltage (Negative Boost): (a) Load voltage, and (b) Load current

The converter response to load variations are shown in Figure 13. The results illustrate the capability of the converter to precisely control the output voltage at 200 % of supply voltage though the large changes in the load.

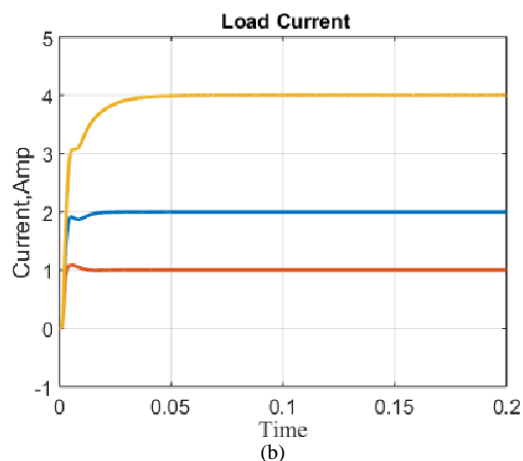
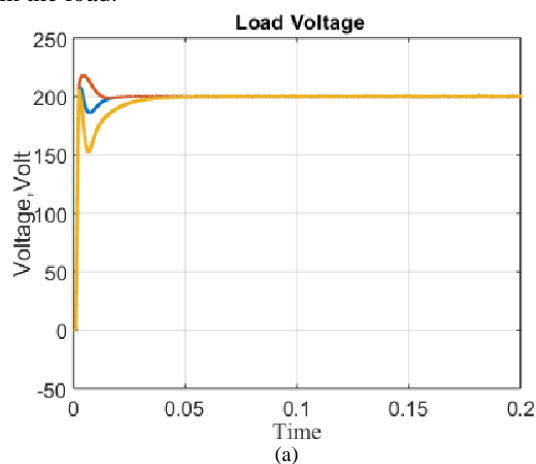


Figure 13-Response to variation in system loads: (a) Load voltage, and (b) Load current.

## 6. Conclusions

The paper presents stability analysis and performance evaluation of a multifunction Converter. A multifunction circuit topology is proposed and a time-invariant state-space model for the converter obtained using state-space average technique. The results indicated show that the converter is a non-minimum phase and an inner loop is required for improved converter performance. Also, the results illustrated that increasing the converter capacitance reduces the stability margin while increasing the inductance reduces the damped frequency. A comprehensive assessment of stability using the frequency domain and pole-zero locus domains that indicated that careful attention should be given to the controller design. The simulation results illustrate successful operation of the converter to satisfy the positive and negative function requirements.

## 7. References

- [1] N. Mohan, "Power Electronics", John Wiley & Sons, Inc., ISBN 978-1-118-07480-0, 2012.
- [2] E. Cipriano Dos Santos Jr., "Advanced power electronics converters", IEEE Press, ISBN: 9781118880944, 2015.
- [3] M. H. Rashid, "Power Electronics: Devices, Circuits and Applications", Pearson Education Limited 2014, ISBN 13: 978-0-273-76908-8, 2014.
- [4] P. Zumel, et al., "Modular Dual-Active Bridge Converter Architecture," in IEEE Transactions on Industry Applications, Vol. 52, No. 3, pp. 2444-2455, May-June 2016.

- [5] M. K. Kazimierczuk, N. Kondrath,: "Comparison of wide- and high-frequency duty-ratio-to-inductor-current transfer functions of dc–dc PWM buck converter in CCM", IEEE Transactions on Industrial Electronics, Vol. 59, No. 1, pp. 641-643, January 2012.
- [6] V. Mummadi, B. Krishna Mohan,: "Robust Digital Voltage Mode Controller for Fifth- Order Boost Converter", IEEE Transactions on Industrial Electronics, Vol. 58, No. 1, pp. 263-277, 2011.
- [7] H. Wu, L. Zhu, F. Yang,: "Three-Port-Converter-Based Single-Phase Bidirectional AC–DC Converter With Reduced Power Processing Stages and Improved Overall Efficiency", IEEE Transactions on Power Electronics, Vol. 33, No. 12, pp. 10021-10026, December 2018.
- [8] S. Lee, K. Kim, J. Kwon, B. Kwon,: "Single-phase transformerless bi-directional inverter with high efficiency and low leakage current", IET Power Electronics, Vol. 7, No. 2, pp. 451-458, 2014.
- [9] H. Chen, A. Prasai, D. Divan,: "Dyna-C: A Minimal Topology for Bidirectional Solid State Transformers", IEEE Transactions on Power Electronics, Vol. 32, No. 2, pp. 995-1005, February 2017.
- [10] H. Fan, H. Li,: "High-Frequency Transformer Isolated Bidirectional DC–DC Converter Modules With High Efficiency Over Wide Load Range for 20 kVA Solid-State Transformer," IEEE Transactions on Power Electronics, Vol. 26, No. 12, pp. 3599-3608, December 2011.
- [11] L. Ma, K. Sun, R. Teodorescu, J. M. Guerrero, X. Jin,: "An Integrated Multifunction DC/DC Converter for PV Generation Systems", IEEE International Symposium on Industrial Electronics, DOI: 10.1109/ISIE.2010.5637648, Bari, Italy, 4-7 July 2010.
- [12] M. Uno, K. Sugiyama,: "Switched Capacitor Converter-Based Multi-Port Converter Integrating Bidirectional PWM and Series-Resonant Converters for Standalone Photovoltaic System", IEEE Transactions on Power Electronics, Vol. 34, No. 2, pp. 1394-1406, February 2019.
- [13] J. Zhang, J. Liu, J. Yang, N. Zhao, Y. Wang, T. Q. Zheng,: "A Modified DC Power Electronic Transformer Based on Series Connection of Full-Bridge Converters", IEEE Transactions on Power Electronics, Vol. 34, No. 3, pp. 2119-2133, 2019.
- [14] A. Emadi,: "Modeling and analysis of multi-converter DC power electronic systems using the generalized state-space averaging method", IEEE Transactions on Industrial Electronics, Vol. 51, No. 3, pp. 661-668, June 2004.
- [15] M. Karppanen, J. Arminen, T. Suntio, K. Savela, J. Simola,: "Dynamical Modelling and Characterization of Peak-current-controlled Super Buck Converter", IEEE Trans. on Power Electron., Vol. 23, No. 3, pp. 1370-1380, May 2008.
- [16] K. Ogata,: "Modern Control Engineering," Prentice Hal , ISBN 13: 978-0-13-615673-4, 2010.